T51H-0390 GNSS-Acoustic Observation Using the Wave Glider to Detect the Seafloor Crustal Deformation Associated with the Temporal Change in the Interplate Locking State

Takeshi Iinuma*[1], Motoyuki Kido[2], Yusaku Ohta[2], Tatsuya Fukuda[1], Fumiaki Tomita[1], Ryota Hino[2], and Iwao Ueki[1]
[1]Japan Agency for Marine-Earth Science and Technology (JAMSTEC)
[2] Tohoku University
*iinuma@jamstec.go.jp

Introduction

- **Periodic changes in the interplate locking** in the northeast Japan subduction zone [Uchida et al., 2016, Science]
  - ✓ The activity of small repeating earthquakes
  - ✓ The terrestrial crustal deformation
    - ▪ The slow slip on the plate interface has occurred repeatedly at intervals of from 2 to 6 years (Fig. 1).
- **Northern part of the Japan Trench**
  - ✓ A tsunami earthquake in 1896 ruptured the shallow plate boundary
    - W The coseismic slip fully released the interseismic slip deficit?
    - W The periodic slow slip events occur near the trench?
      - ⇨ A research project: "**Head and tail of massive earthquakes: Mechanism arresting growth of interplate earthquakes**" (JSPS KAKENHI Grant Number JP19H05596)
        - ▪ **Frequent GNSS-Acoustic observation is essential!**
- **Automatic GNSS-A data acquisition system** using an unmanned surface vehicle, the **Wave Glider**, is developed to overcome the high cost of the research vessel as the sea-surface platform.

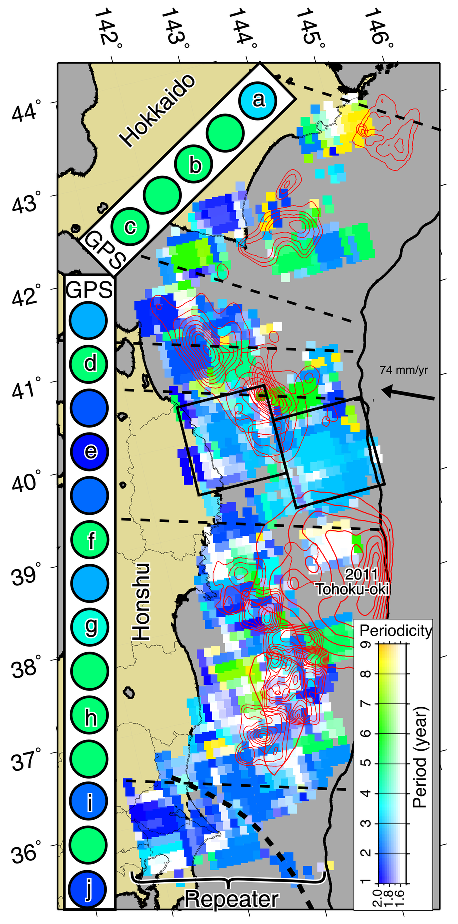

Fig. 1 (Fig. 4 of Uchida et al. [2016]): Spatial distribution of degree of periodicity (color intensity) and dominant period (color) estimated from the repeater data for the periods from 1984 to 2011 (between 36.5° N and 41.5° N) and from 1993 to 2011 (north of 41.5° N and south of 36.5° N). The periods indicated for each area represent the dominant peak in the amplitude spectrum of the slip velocity variations inferred from repeaters for 0.4° (lat.) by 0.6° (lon.) spatial windows. Contours show slip areas for the 2011 Tohoku-oki earthquake (M9.0) and other M7 or larger earthquakes since 1930. Colored circles show dominant period of on-land GPS gradient in plat1motion parallel to N105° E (Honshu) and N120° E (Hokkaido) directions.

Automatic GNSS-A Observation System

- **Wave Glider (Sv3)**
  - ✓ Composed of sea-surface "**Float**" and "**Glider**" in the water
- **Float**
  - ✓ Command and Control Unit (CCU) handling......
    - ▪ Iridium satellite communication
    - ▪ Wi-Fi communication
    - ▪ AIS (Automatic Identification System)
  - ✓ Power generation and consumption
    - ▪ Solar panels generate 156 W at the maximum.
    - ▪ Battery capacity: 1820 Wh at the maximum
    - ▪ Power consumption for cruising: less than 10 W
    - ▪ GNSS-A Observation equipments in the waterproof container consumed ~24.5 W at the maximum (~ 600 W/day).
      - GNSS Antennas
      - GNSS Receiver
      - MEMS Gyroscope
      - Acoustic Unit
      - Acoustic Transducer
      - Controlling / Recording PC
      - Wi-Fi Router to communicate the devices in the container
      - Power supply circuit board
- **Glider**
  - ▪ Wing to generate the driving force (Fig. 4)
  - ▪ Rudder to direct the course
  - ▪ Auxiliary thruster: consuming 50 Wh at the maximum

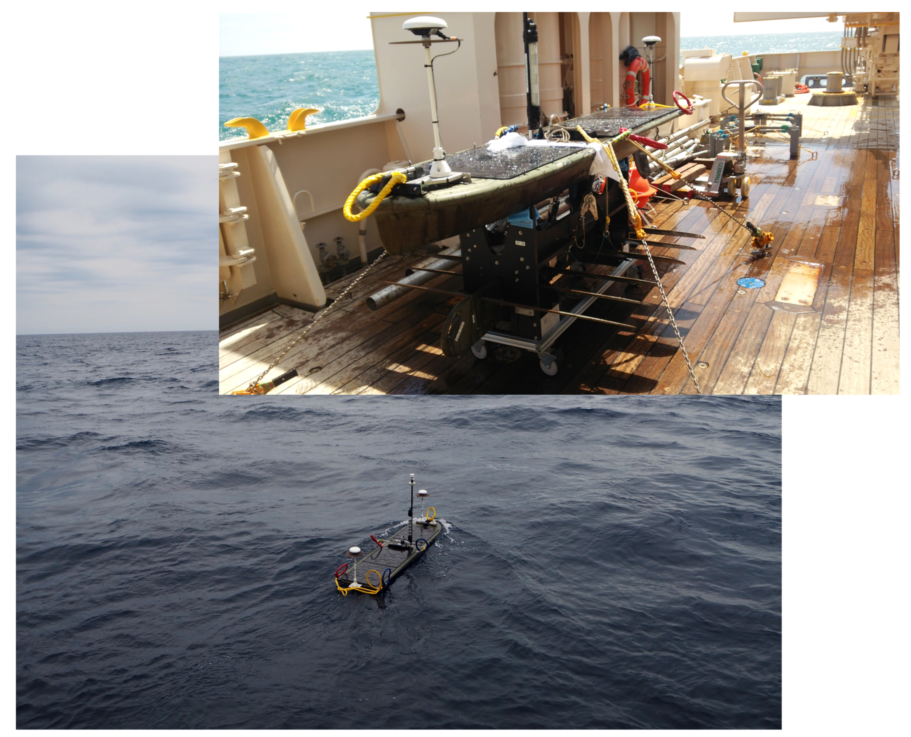

Fig. 2. Wave Glider used during the cruise KS-19-12

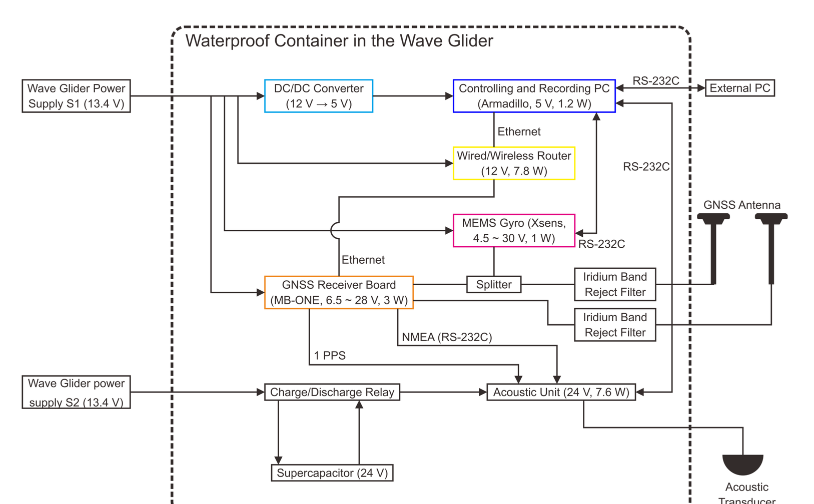

Fig. 3. Block diagram of the GNSS-A observation system mounted on the Wave Glider

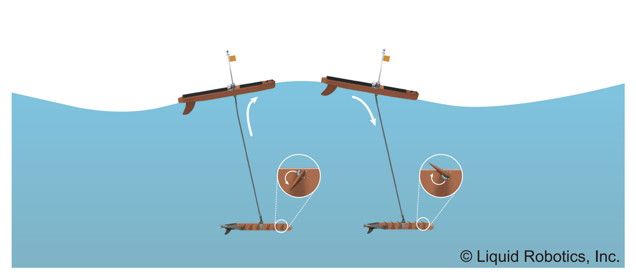

Fig. 5. Schematic figure how to work the Wave Glider. "Glider" advances by converting the up-down motion due to the sea surface wave and float buoyancy into the advancing force.

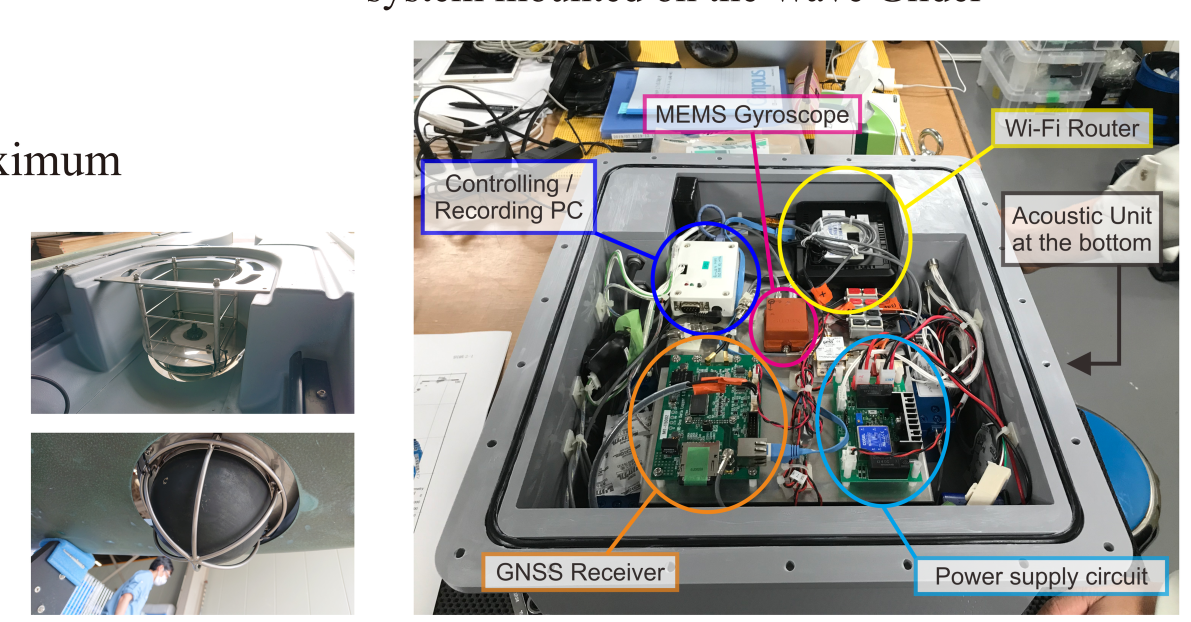

Fig. 4. Acoustic transducer mounted close to the stern and the observation devices installed in the waterproof container

Observation Cruise (KS-19-12, Research Vessel "Shinsei-maru")

First test of the automatic GNSS-A observation system

At site G02 off Aomori Prefecture
- ✓ Installed in 2012
- Test items
  - ✓ The data acquisition from the sensors
    - ▪ GNSS carrier phase
    - ▪ Attitude (heading, roll and pitch)
    - ▪ Acoustic wave from the transponders
  - ✓ Autonomous activation of the seafloor transponders
    - ▪ by turning the power supply to the payload on/off from land via a satellite communication

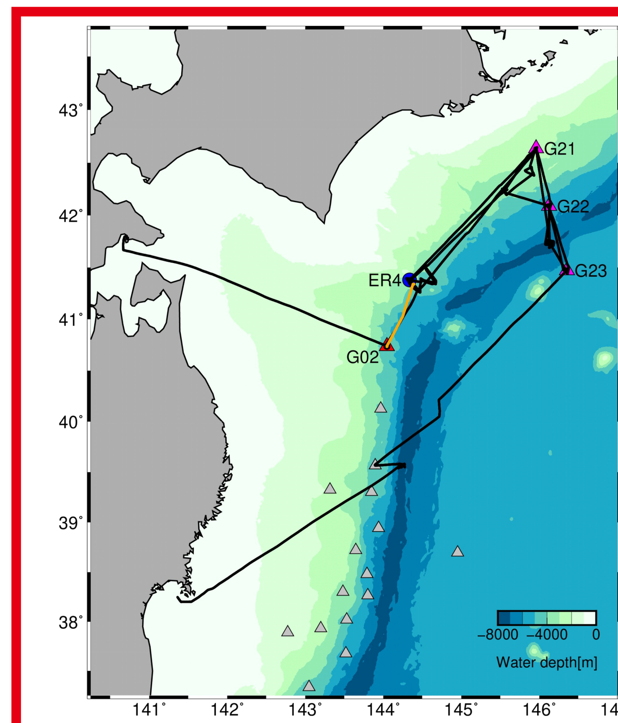

Fig. 6. Tracks of the Wave Glider and **Shinsei-maru**

Cruise Itinerary (Time is in GMT)

- July 3, 05:00, Departure from Hakodate
- July 3, 23:50, Deployment of the Wave Glider at G02
- July 4, 03:00, Shinsei-maru left G02.
- July 5, 08:17, Suspension of the observation
  Seafloor stations went into "sleep mode" after 1 hour.
- July 5, 23:00, Resumption of the observation
  Activation of the seafloor stations was automatically executed.
- July 6, 04:32, The Wave Glider left G02.
- July 7, 16:00, The Wave Glider arrived at the retrieval point ER4.
- July 7, 23:00, Retrieval operation began.
- July 7, 23:58, Retrieval operation completed.

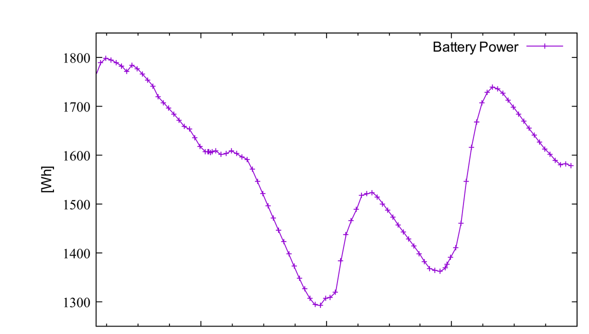

Fig. 7. Trend of the total battery power of the Wave Glider

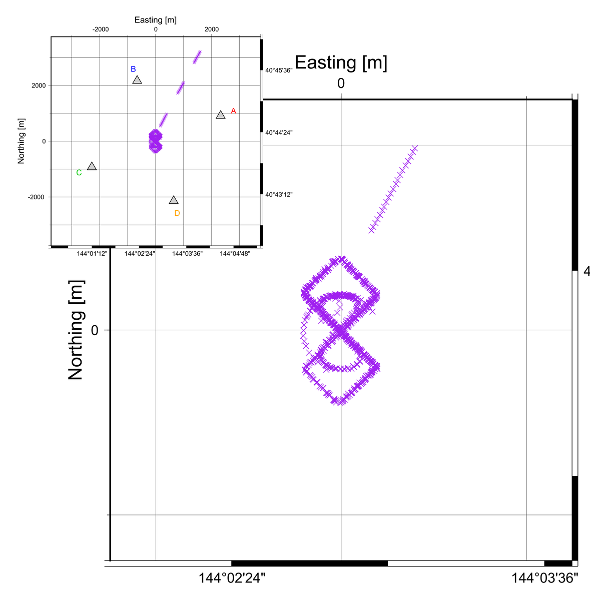

Fig. 8. Locations of the Wave Glider at the timing of acoustic shots

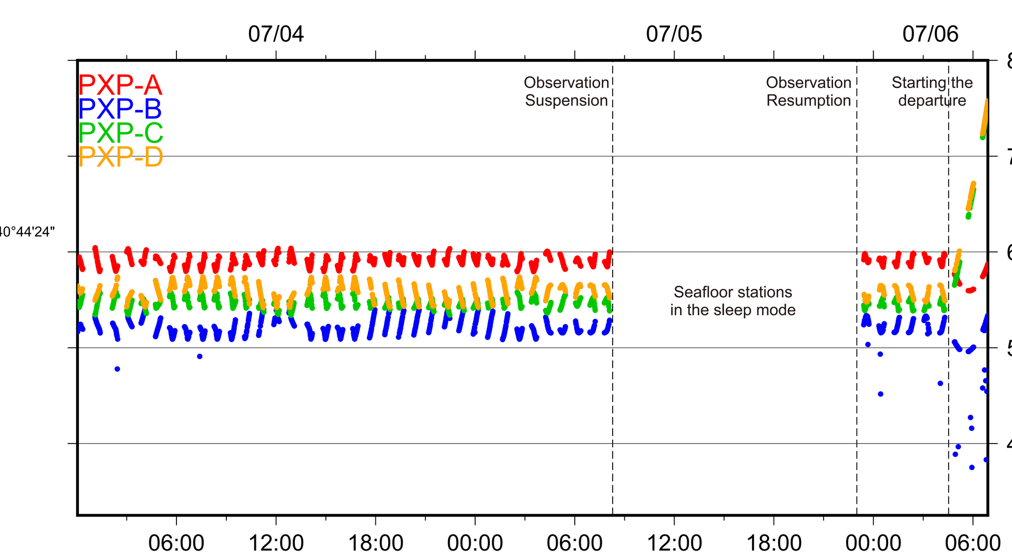

Fig. 9. Time series of the slant ranges between the Wave Glider and seafloor stations.

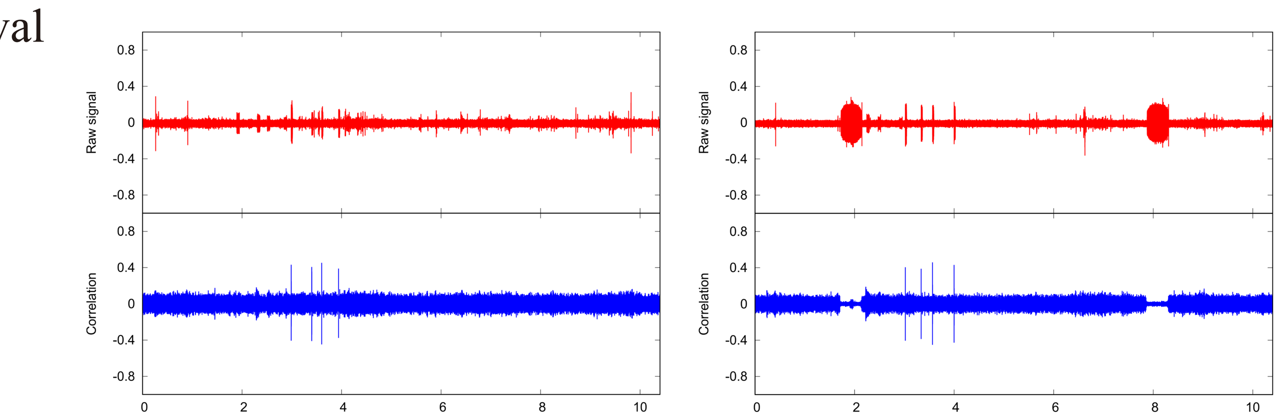

Fig. 10. Examples of the raw acoustic waveform (upper panels) and the correlation waveform between the transmitted code (lower panels).

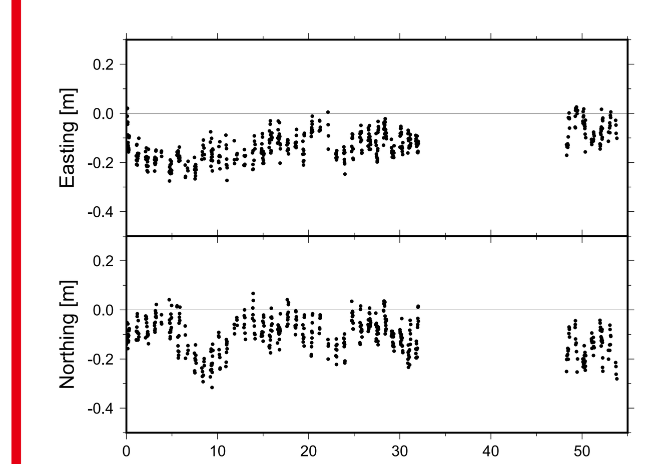

Fig. 11. Time series of the estimated position of the array center for each acoustic shot. (Upper) East-west and (lower) North-south components are exhibited.

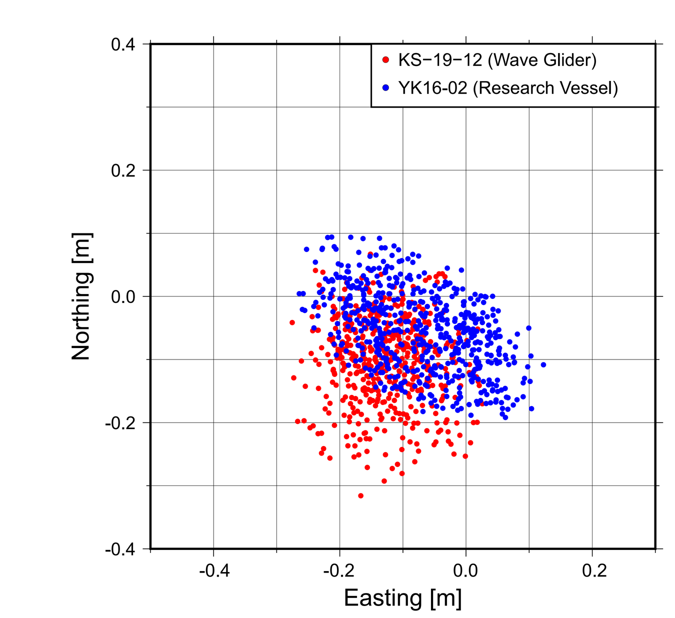

Fig. 12. Estimated position of the array center for each shot. Red and blue dots show the positions based on the data obtained by using the Wave Glider and a research vessel "YOKOSUKA".

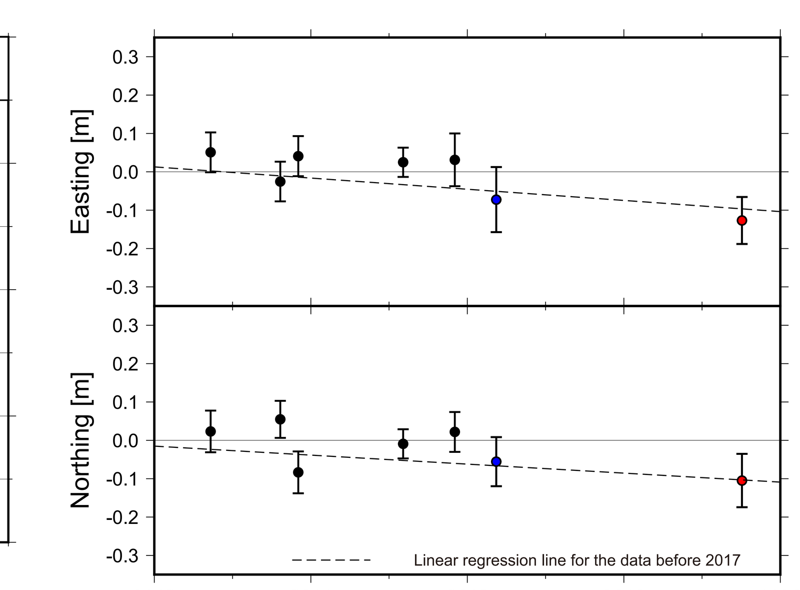

Fig. 13. Time series of the averaged array center positions. (Upper) East-west and (lower) north-south components are plotted. The broken lines correspond with the displacement rate estimated from data before 2017.

Summary of the Observation Results

- The automatic control of the observation system is succeeded.
  - ✓ Automatic navigation of the Wave Glider and power management (Figs. 6-8).
  - ✓ Wave-up of the seafloor stations and data acquisition (Figs. 8 and 9).
- The quality of the observed data is sufficient to estimate the seafloor crustal deformation (Figs. 10 and 11).
  - ✓ The error of the array position is almost the same degree with that based on the research vessels' data (Fig. 12).
  - ✓ Estimated array position is consistent with the past data and averaged displacement rate based on them (Fig. 13).
- Next Step
  - ✓ Longer operation (~ a month)
  - ✓ Realtime estimation of the seafloor crustal deformation